Available online at www.sciencedirect.com
SCIENCE DIRECT®
Surface Science 566–568 (2004) 659–663
SURFACE SCIENCE
www.elsevier.com/locate/susc

Low-dimensional hybrid organic–inorganic nanostructures via planar DNA–amphiphilic polycation complexes

A.N. Sergeev-Cherenkov [a], M.N. Antipina [a], T.V. Yurova [a], A.A. Rakhnyanskaya [b], R.V. Gainutdinov [c], A.L. Tolstikhina [c], V.V. Kislov [d], G.B. Khomutov [a,*]

[a] *Faculty of Physics, Moscow State University, 119992 Moscow, Russia*
[b] *Department of Chemistry, Moscow State University, 119992 Moscow, Russia*
[c] *Institute of Crystallography RAS, 119899 Moscow, Russia*
[d] *Institute of Radioengineering and Electronics RAS, 125009 Moscow, Russia*

Available online 11 June 2004

Abstract

New nanoscale organized planar complexes of DNA and amphiphilic polycation on the surfaces of solid substrates were obtained via the formation of Langmuir monolayer at the gas–aqueous phase interface composed by water-insoluble amphiphilic polycation poly(4-vinylpyridine) with 16% cetylpyridinium groups, then binding of DNA molecules from the aqueous phase with the amphiphilic polycation monolayer, and, finally, deposition of the planar complex structure. Those monolayer and multilayer DNA/polycation complex Langmuir–Blodgett films were used as nanotemplates and nanoreactors for synthesis of inorganic nanostructures. The obtained nanostructures were characterized by atomic force microscopy and transmission electron microscopy techniques. As a result, ultrathin planar polymeric nanocomposite films with integrated DNA molecules and organized inorganic semiconductor CdS and iron oxide nanoparticle quasi-linear arrays were formed successfully.

Keywords: Atomic force microscopy; Scanning transmission electron microscopy (STEM); Biological molecules – nucleic acids; Surface structure, morphology, roughness, and topography; Clusters; Iron oxide; Cadmium sulphide; Liquid–gas interfaces

1. Introduction

Clusters, nanoparticles, nanorods and nanowires, long molecules as nanotubes and polynucleotides are currently considered as potential functional and structural building blocks for new advanced nanostructured materials, films, devices and circuits for nanoelectronics and nanotechnological (including nanobiotechnology) applications. The development and introduction of new low-cost methods with effective control of their structure, composition and purposeful nanoscale assembly and organization are now necessary. Fabrication of organized low-dimensional structures composed of nanoscale functional components is a principal step on the way of practical

* Corresponding author. Tel.: +7-095-939-3025; fax: +7-095-939-1195.
E-mail address: GBK@phys.msu.ru (G.B. Khomutov).

0039-6028/$ - see front matter © 2004 Elsevier B.V. All rights reserved.
doi:10.1016/j.susc.2004.05.126

manufacturing of nanodevices. Langmuir–Blodgett (LB) technique was proven to be an effective tool for fabrication of organized two-dimensional arrays of nanoclusters, proteins, nanoparticles and nanowires [1–6]. It is substantially more difficult to form reproducibly one-dimensional chain structures from nanoparticles, however, this task was solved successfully by nature. Various magnetotactic bacteria can synthesize fine (40–100 nm) ferromagnetic crystalline iron oxide particles (Fe_3O_4 with a small admixture of γ-Fe_2O_3 phase) forming magnetosome structures in which membrane-bound magnetic nanoparticles are organized and arranged in regular chains [7,8]. The chain magnetosome structures play important physiological role in bacteria giving them possibilities for orientation in the earth's magnetic field. There is an approach to formation of self-organized one-dimensional inorganic nanostructures (chains of nanoparticles and nanowires) based on the use of polymeric molecules (in particularly, DNA) as templates. One-dimensional metallic nanostructures (chains of Pt nanoparticles [9], silver [10] and gold [11] metallic nanowires), cadmium sulfide nanoparticles [12–14] and DNA–magnetite nanocomposite [15] were fabricated via DNA templating and stabilizing. Starting from the pioneering work [16], atomic force microscopy (AFM) was widely used for investigation of immobilized DNA molecules and complexes.

Recently, we have developed an approach to fabrication of new nanoscale-organized planar DNA complexes with amphiphilic polycations using LB technique [17]. In our present work the monolayer and multilayer DNA/amphiphilic polycation complex LB films on the surface of solid substrates were formed, characterized and used as nanotemplates and nanoreactors for generation of organized inorganic (iron oxide and semiconductor) nanostructures. We were interested in investigation of effects of nanoscale organization of inorganic nanostructures generated in low-dimensional organized polymeric matrix. The morphology of obtained nanocomposite particulate film was studied, and AFM and transmission electron microscopy (TEM) techniques were used to characterize the fabricated nanostructures.

2. Experimental details

Salmon thimus native DNA (Na salt) and arachidic acid (AA) were obtained from Sigma. Milli-Q water purification system was used to produce water with resistivity about 18 MΩ cm. Surface pressure–monolayer area isotherm measurements, monolayer formation and deposition onto the solid substrates were carried out on a fully automatic conventional Teflon trough at 21 °C as described elsewhere [18]. *N*-alkylated derivatives of poly(4-vinilpyridine) (PVP) were used as water-insoluble amphiphilic polycations to form polymeric monolayer and novel planar DNA/amphiphilic polycation complexes at the air–aqueous DNA solution interface. Linear charge density as well as hydrophilic–lipophilic (hydrophobic) balance of such molecules can be easily controlled by varying the extent of *N*-alkylation and the nature of alkyl groups. Water-insoluble amphiphilic polycation poly-4-vinylpyridine with 16% cetylpiridinium groups (PVP-16) was synthesized via the known procedures [19]. To obtain amphiphilic polycation PVP fraction with degree of polymerization 1100 was prepared and then quaternized with cetyl bromide as described in [20]. Langmuir monolayer of PVP-16 molecules on the surface of aqueous DNA solution was formed using spreading solution of PVP-16 in chloroform (concentration 10^{-4} M for monomer). Planar DNA complexes with amphiphilic polycation were formed as described in [17].

Mica substrates were used for AFM investigations and were freshly cleaved immediately before monolayer deposition. Samples for TEM measurements were prepared by monolayer deposition from aqueous subphase surface onto the Formvar film supported by the copper grid. Iron oxide nanoparticles were generated via the incubation of corresponding precursor film containing Fe^{3+} cations (Ferrous arachidate LB film and DNA/Fe^{3+}/PVP-16 complex film) in the sodium borohydride (5×10^{-4} M) solutions to form mixed Fe^{2+}/Fe^{3+} compositions in the films followed by the film incubation in the high pH aqueous media (pH = 10) at ambient conditions for 1 or 2 h. The preliminary analyses of the generated iron-containing nanoparticles using electron diffraction

technique pointed to the iron oxide nature (magnetite and maghemite phases) of obtained nanoparticles. Fe^{3+}-containing five-layer AA LB films were formed by the vertical lifting deposition of arachidic acid monolayer from the $FeCl_3$ solution (2×10^{-4} M, pH = 2.5) onto the substrate surface. DNA/Fe^{3+}/PVP-16 complex film was formed via the incubation of DNA/PVP-16 LB film in the $FeCl_3$ solution (2×10^{-4} M, pH = 2.5). CdS nanoparticles and nanowires were synthesized via the incubation of corresponding precursor film containing Cd^{2+} cations (DNA/Cd^{2+}/PVP-16 complex film) in the H_2S atmosphere for 2 h. DNA/Cd^{2+}/PVP-16 complex film was formed via the incubation of DNA/PVP-16 LB film in the $CdCl_2$ solution (2×10^{-4} M, pH = 6.0) for 1 h.

AFM measurements were performed with the use of Solver P47-SPM-MDT scanning probe microscope (NT MDT Ltd., Moscow, Russia) in a tapping mode. Silicon cantilevers NSC11 (Estonia, Mikromasch) with tip-radii of about 10 nm were used. Images were measured in air at ambient temperature (21 °C) and were stable and reproducible.

TEM images were obtained with the use of Jeol JEM-100B microscope.

3. Results and discussion

Fig. 1 shows AFM top view topographic images of PVP-16 and complex DNA/PVP-16 LB films deposited onto the mica substrate (Fig. 1a and Fig. 1b–d, correspondingly). Nanoscale-ordered planar structure of PVP-16 film is clearly seen from the Fig. 1a. Efficient electrostatic repulsive interactions in amphiphilic polyelectrolyte Langmuir monolayer play apparently important role in the formation of regular structure of deposited polymeric films. The characteristic morphologies of DNA/PVP-16 complexes which can be obtained in dependence on the amphiphilic polycation monolayer state during the DNA binding are presented on the Fig. 1b (extended planar net-like structure) and Fig. 1d) (quasi-circular toroidal structure). Individual DNA molecules also were observed (Fig. 1c).

Fig. 2 shows TEM micrographs with iron oxide and cadmium sulfide nanoparticles and nanostructures generated in multilayer DNA/PVP-16 complex LB films. For comparison, iron oxide nanoparticles formed in multilayer ferrous arachidate LB film via the same synthetic procedure are shown on the Fig. 2a. One can see that important feature of images with nanoparticles generated in DNA/PVP-16 complex film is the organized character of nanoparticles arrangement in the film. In contrast to rather random and disordered arrangement of iron oxide nanoparticles in AA LB film (although, some tight chains are present possibly due to the dipole–dipole attraction of magnetic iron oxide nanoparticles) on the Fig. 2a, nanoparticles on the Fig. 2b, c and e are predominantly organized as quasi-linear chain structures.

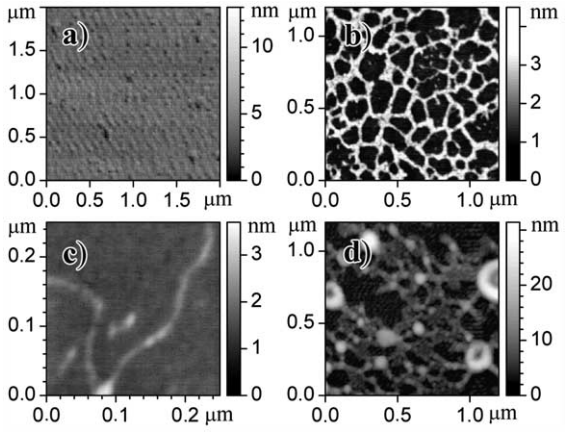

Fig. 1. AFM tapping mode images of two-layer LB films deposited onto the mica substrate. (a) Top view topographic image of PVP-16 LB film deposited after 10 min incubation of the PVP-16 Langmuir monolayer at low surface pressure value ($\pi \cong 0$) on the water subphase surface (pH = 6) (image size 2 μm × 2μm, black-to-white color height scale is 0–13 nm). (b) Top view topographic images of DNA/PVP-16 complex LB film. Complex formation conditions: PVP-16 monolayer surface pressure value ~0 during the DNA binding, incubation time 25 min. The composition of the aqueous subphase was 1.2×10^{-4} M DNA (for monomer), 1 mM NaCl, pH = 6 (image size: 1.2 μm × 1.2 μm, black-to-white color height scale is 0–4.2 nm). (c) Single DNA molecule bound with PVP-16 monolayer, image size: 0.22 μm × 0.22 μm, black-to-white color height scale is 0–3.5 nm. (d) Top view topographic images of DNA/PVP-16 complex LB film. Complex formation conditions: PVP-16 monolayer surface pressure value 20 mN/m during the DNA binding, incubation time 25 min on the surface of aqueous subphase with composition: 1.2×10^{-4} M DNA (for monomer), 1 mM NaCl, pH = 6 (image size 1.2 μm × 1.2 μm, black-to-white color height scale is 0–30 nm).

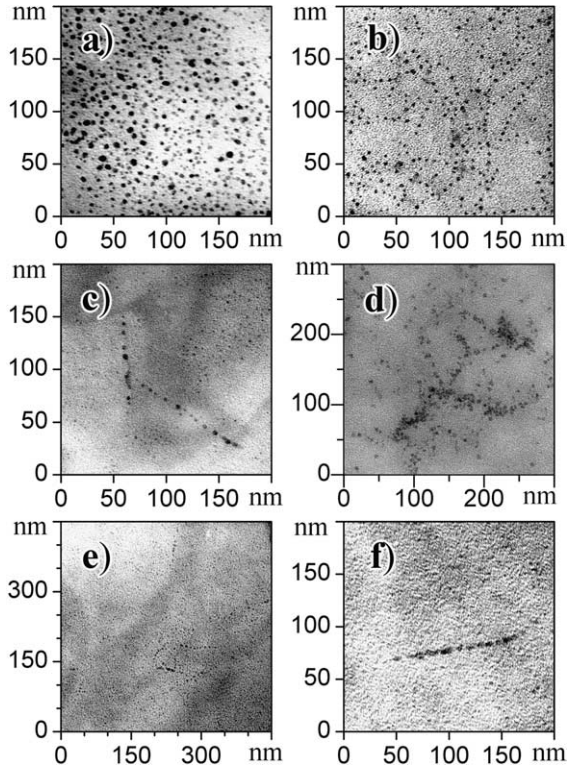

Fig. 2. Transmission electron micrographs showing iron oxide and cadmium sulphide nanoparticles in fabricated hybrid organic–inorganic nanostructures. (a) Iron oxide nanoparticles synthesized in multilayer ferrous arachidate LB film with $NaBH_4$ (5×10^{-4} M) used as a reductant. (b) Iron oxide nanoparticles synthesized in planar DNA/Fe^{3+}/PVP-16 complex LB films (incubation time 1 h). (c) Iron oxide nanoparticles synthesized in planar DNA/Fe^{3+}/PVP-16 complex LB films (incubation time 2 h). (d) Iron oxide nanoparticles synthesized in planar DNA/Fe^{3+}/PVP-16 complex LB films (incubation time 2 h). (e) CdS nanoparticles grown in DNA/Cd^{2+}/PVP-16 complex LB film. (f) CdS nanowire grown in DNA/Cd^{2+}/PVP-16 complex LB film.

Aggregation and coalescence of adjacent nucleus and nanoparticles in linear structures of DNA complexes can result in formation of nanorods and nanowires (Fig. 2c and f). Also, aggregates of iron oxide nanoparticles (Fig. 2d) similar in morphology to the net-like DNA/PVP-16 complex film structures (image Fig. 1b) were also observed giving evidence for important role of the fine structure of polymeric complex film and, particularly of DNA molecules, in organization of grown

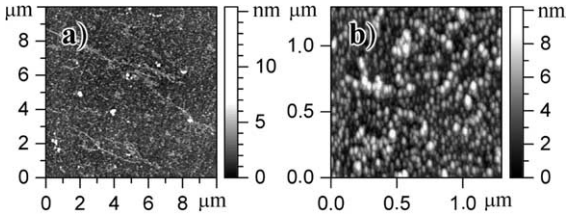

Fig. 3. AFM tapping mode top view topographic images of nanoparticulate DNA/PVP-16 complex five-layer LB film on the mica substrate corresponding to the sample presented on images (c) and (d) of the Fig. 2. (a) Image size: 10 μm × 10 μm, black-to-white color height scale is 0–15 nm. (b) Image size: 1.3 μm × 1.3 μm, black-to-white color height scale is 0–10 nm.

nanoparticles. The mean diameter of iron oxide nanoparticles generated in DNA/PVP-16 complex film was about 2.5 nm. Such small iron oxide nanoparticles may be perspective for nanoelectronic applications because single-electron tunneling effects can be observed in such nanoparticles at room temperature [21].

Fig. 3 shows AFM top view topographic images of nanoparticulate DNA/PVP-16 complex five-layer LB film on the mica substrate corresponding to the sample presented on c and d of the Fig. 2. One can see the presence of extended (Fig. 3a) and net-like (Fig. 3b) morphologies in the structure of surface of nanoparticulate complex film. The last observation can reflect the correspondence of morphology of extended DNA complexes on Fig. 1 with structure of quasi-linear and net-like arrays of iron oxide nanoparticles on Fig. 2. More pronounced granular structure of the LB film on Fig. 3 can be a result of increased number of layers in the film in comparison with Fig. 1. Also, structural changes in amphiphilic polycation–DNA complex film are possible due to the Fe^{3+} binding and following procedures of synthesis of iron oxide nanoparticles. At the same time, homogeneous planar structure of the nanoparticulate DNA/amphiphilic polycation nanocomposite film was not destroyed after the synthesis of nanoparticles.

4. Conclusions

We demonstrate the formation of new planar polymeric composite bio-hybrid complex films

with organized integrated DNA and nanosize inorganic components as semiconductor CdS and iron oxide nanoparticles, and one-dimensional arrays of nanoparticles. The data obtained indicate that the nanoparticle synthetic procedures do not destroy the polymeric matrix of the nanocomposite film. The obtained planar DNA-based polymeric complex and nanocomposite structures with nanoscale structural ordering can be perspective for fabrication of new controlled-morphology ultimately thin organized planar polymeric nanocomposite films and coatings with thickness down to a monolayer for applications in nanoelectronics and nanobiotechnology.

Acknowledgements

This work was supported by Russian Foundation for Basic Researches (Grant 02-03-33158), INTAS (Grant 99-864), ISTC (Grant 1991).

References

[1] S. Boussaad, L. Dziri, R. Arechabaleta, N.J. Tao, R.M. Leblanc, Langmuir 14 (1998) 6215.
[2] S. Henrichs, C.P. Collier, R.J. Saykally, Y.R. Shen, J.R. Heath, J. Am. Chem. Soc. 122 (2000) 4077.
[3] F.C. Meldrum, N.A. Kotov, J.H. Fendler, J. Phys. Chem. 98 (1994) 4506.
[4] G.B. Khomutov, L.V. Belovolova, S.P. Gubin, V.V. Khanin, A.Yu. Obydenov, A.N. Sergeev-Cherenkov, E.S. Soldatov, A.S. Trifonov, Bioelectrochemistry 55 (2002) 177.
[5] G.B. Khomutov, R.V. Gainutdinov, S.P. Gubin, A.Yu. Obydenov, A.N. Sergeev-Cherenkov, V.V. Shorokhov, E.S. Soldatov, A.L. Tolstikhina, A.S. Trifonov, Surf. Sci. 532–535 (2003) 287.
[6] D. Whang, S. Jin, Y. Wu, C.M. Lieber, Nanoletters 3 (2003) 1255.
[7] D. Schuler, R.B. Frankel, Appl. Microbiol. Biotechnol. 52 (1999) 464.
[8] R.B. Frankel, R.P. Blakemore, R.S. Wolfe, Science 203 (1979) 1355.
[9] M. Mertig, L.C. Ciacchi, R. Seidel, W. Pompe, Nanoletters 2 (2002) 841.
[10] J.J. Storhoff, C.A. Mirkin, Chem. Rev. 99 (1999) 1849.
[11] O. Harnack, W.E. Ford, A. Yasuda, J.M. Wessels, Nanoletters 2 (2002) 919.
[12] J.L. Coffer, S.R. Bigham, R.F. Pinizzotto, H. Yang, Nanotechnology 3 (1992) 69.
[13] R. Mathab, J.P. Rogers, C.P. Singleton, C.J. Murphy, J. Am. Chem. Soc. 117 (1996) 7028.
[14] J.L. Coffer, S.R. Bigham, X. Li, R.F. Pinizzotto, Y.G. Rho, R.M. Pirtle, I.L. Pirtle, Appl. Phys. Lett. 69 (1996) 3851.
[15] S. Mornet, A. Vekris, J. Bonnet, E. Duguet, F. Grasset, J.-H. Choy, J. Portier, Mater. Lett. 42 (2000) 183.
[16] P.K. Hansma, V.B. Elings, O. Marti, C.E. Bracker, Science 242 (1988) 209.
[17] M.N. Antipina, R.V. Gainutdinov, A.A. Rachnyanskaya, A.L. Tolstikhina, T.V. Yurova, G.B. Khomutov, Surf. Sci. 532–535 (2003) 1025.
[18] S.A. Yakovenko, V.V. Kislov, V.V. Erokhin, A.Yu. Popatov, G.B. Khomutov, Russ. J. Phys. Chem. (English Translation) 66 (1992) 541.
[19] A.A. Yaroslavov, E.G. Yaroslavova, A.A. Rakhnyanskaya, F.M. Menger, V.A. Kabanov, Colloid Surf. B 16 (1999) 29.
[20] R.M. Fuoss, U.P. Strauss, J. Polym. Sci. 3 (1948) 246.
[21] R.G.C. Moore, S.D. Evans, T. Shen, C.E.C. Hodson, Physica E 9 (2001) 253.